



Cite this: *Chem. Commun.*, 2023, 59, 2571

# Surface chemistry and structure manipulation of graphene-related materials to address the challenges of electrochemical energy storage

Yue Sun,<sup>a</sup> Jinhua Sun,<sup>\*b</sup> Jaime S. Sanchez,<sup>c</sup> Zhenyuan Xia,<sup>b,d</sup> Linhong Xiao,<sup>e</sup> Ruiqi Chen<sup>b</sup> and Vincenzo Palermo<sup>b,\*bd</sup>

Energy storage devices are important components in portable electronics, electric vehicles, and the electrical distribution grid. Batteries and supercapacitors have achieved great success as the spearhead of electrochemical energy storage devices, but need to be further developed in order to meet the ever-increasing energy demands, especially attaining higher power and energy density, and longer cycling life. Rational design of electrode materials plays a critical role in developing energy storage systems with higher performance. Graphene, the well-known 2D allotrope of carbon, with a unique structure and excellent properties has been considered a “magic” material with its high energy storage capability, which can not only aid in addressing the issues of the state-of-the-art lithium-ion batteries and supercapacitors, but also be crucial in the so-called post Li-ion battery era covering different technologies, e.g., sodium ion batteries, lithium–sulfur batteries, structural batteries, and hybrid supercapacitors. In this feature article, we provide a comprehensive overview of the strategies developed in our research to create graphene-based composite electrodes with better ionic conductivity, electron mobility, specific surface area, mechanical properties, and device performance than state-of-the-art electrodes. We summarize the strategies of structure manipulation and surface modification with specific focus on tackling the existing challenges in electrodes for batteries and supercapacitors by exploiting the unique properties of graphene-related materials.

Received 12th December 2022,  
Accepted 20th January 2023

DOI: 10.1039/d2cc06772b

[rsc.li/chemcomm](http://rsc.li/chemcomm)

<sup>a</sup> Key Laboratory of Green and Precise Synthetic Chemistry and Applications, Ministry of Education, College of Chemistry and Materials Science, Huaibei Normal University, Huaibei, Anhui 235000, P. R. China

<sup>b</sup> Department of Industrial and Materials Science, Chalmers University of Technology, SE-412 96 Göteborg, Sweden. E-mail: [jinhua@chalmers.se](mailto:jinhua@chalmers.se)

<sup>c</sup> Electrochemical Processes Unit, IMDEA Energy Institute, Avda. Ramon de la Sagra 3, Parque Tecnológico de Mostoles, 28935, Mostoles, Spain

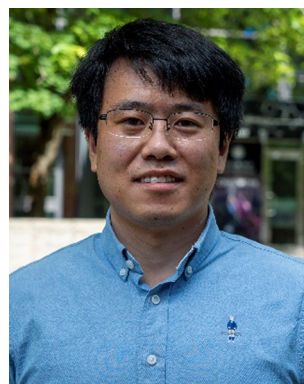
<sup>d</sup> Institute for Organic Synthesis and Photoreactivity (ISOF), National Research Council of Italy (CNR), Via P. Gobetti 101, I-40129 Bologna, Italy. E-mail: [vincenzo.palermo@isof.cnr.it](mailto:vincenzo.palermo@isof.cnr.it)

<sup>e</sup> Department of Organismal Biology, Uppsala University, SE-752 36 Uppsala, Sweden



**Yue Sun**

*Dr Yue Sun is currently an associate professor at College of Chemistry and Materials Science, Huaibei Normal University. He received his BEng degree from China University of Mining & Technology, Beijing in 2015. He then received his PhD degree in Chemistry and Physics of Polymers from the Technical Institute of Physics and Chemistry (TIPC), Chinese Academy of Sciences (CAS) in 2020. His current research interest is focused on bioinspired porous materials for energy conversion and storage.*



**Jinhua Sun**

*Dr Jinhua Sun is currently an Oavlönad docent at Chalmers University of Technology. He received his PhD degree in Chemistry and Physics of Polymers from Technical Institute of Physics and Chemistry (TIPC), Chinese Academy of Sciences (CAS) in 2016. Aferward, he did a Postdoc at Umeå University (2016–2018) and Chalmers University of Technology (2018–2020). His research interests are focused on the synthesis of multi-functional materials and development of new technologies for energy related applications.*



# 1. Introduction

With a sharp increase in energy demands and environmental concerns, we need to develop advanced energy conversion and storage technologies to utilize at best renewable energy sources. Energy storage devices play an important role in storing the intermittent energy supply in a wide range of applications from portable electronics, to transport systems, to energy grids.<sup>1</sup> Rechargeable batteries and electrochemical capacitors are the most widely used electrochemical energy storage technologies. Batteries generate energy chemically through electrochemical reactions, also known as non-capacitive faradaic/redox reactions, that occur when the device terminals are connected to an external load. Supercapacitors (SCs), on the other hand, store charge physically through electrostatic interactions at the electrode interfaces with the formation of the electric double layers

(EDLs). Pseudocapacitive effects, due to a limited but fast charge transfer between the electrolyte and electrodes, can also play a significant complementary role in so-called pseudocapacitor devices. All these processes depend on the electrical conductivity, surface chemistry, porous structure and surface area of the electrode materials, which ultimately define the electrochemical energy storage performance for batteries, SCs and pseudocapacitors.<sup>2</sup>

Lithium ion batteries (LIBs) are the current state-of-the-art batteries due to their excellent performance. However, the limited capacity of graphite anodes (theoretical capacity 372 mA h g<sup>-1</sup>), high cost of Li/Co/Ni mineral and lower safety of organic electrolytes result in the demand for alternative energy storage devices. Sodium ion batteries (SIBs), lithium-sulfur (Li-S) batteries, rechargeable Zn-air batteries (ZABs), structural batteries and hybrid SCs or hybrid energy storage devices have



**Jaime S. Sanchez**

*Jaime S. Sánchez is Senior Scientist at SMOLTEK. He holds a PhD degree in the field of Electrochemistry and Materials Science by University of Madrid/IMDEA Energy (2019) focused on the synthesis of graphene-based materials and their application in electrochemical energy storage devices. After his PhD, he joined the 2D-materials group of Vincenzo Palermo at Chalmers University of Technology (Gothenburg, Sweden), where he developed composites for energy storage applications. Currently, he is working at SMOLTEK Hydrogen, developing low-iridium loading PEM water electrolyzers.*



**Zhenyuan Xia**

*Zhenyuan Xia is currently a researcher (Docent) at Chalmers University of Technology and ISOF-Consiglio Nazionale delle Ricerche. He obtained his PhD from East China University of Science and Technology (ECUST) in 2010 and then worked with Dr Vincenzo Palermo's group at ISOF-CNR (Italy) as a Marie-Curie postdoctoral researcher from 2011–2013. His research interests are focused on electrochemical functionalization of graphene-related 2D materials for energy conversion and remediation of organic contaminants.*



**Linhong Xiao**

*Dr Linhong Xiao is a researcher at Uppsala University (Sweden). After receiving her PhD from the Technical Institute of Physics and Chemistry, Chinese Academy of Sciences in 2017, she pursued postdoctoral research in environmental chemistry at Umeå University (Sweden). Linhong is passionate about materials science, environmental chemistry and toxicology.*



**Vincenzo Palermo**

*Vincenzo Palermo is the director of the CNR Institute for Organic Synthesis and Photoreactivity (ISOF) in Bologna, Italy, and an associated professor at Chalmers University of Technology (Sweden). He previously worked at the University of Utrecht (the Netherlands) and at Steacie Institute, National Research Council (Ottawa, Canada). He has been the vice-director of the Graphene Flagship. He uses nanotechnology and chemistry to create new materials for electronics, aerospace and biomedical applications collaborating with key industrial partners in Europe (Airbus, Stellantis, Leonardo etc.). His research interests include supramolecular chemistry, energy storage, composites, water purification and biosensors.*



been considered some of the most promising next-generation energy storage devices to replace or complement LIBs. First, SIBs show huge potential for large-scale energy storage due to their high reliability and the abundance/low cost of sodium. The working mechanism of SIBs is similar to that of LIBs, which is beneficial for mass production of SIBs using well-developed LIB based battery manufacturing technologies. The current issues associated with SIBs are the large size of sodium ions ( $r = 1.02 \text{ \AA}$ ), sluggish interfacial kinetics, unstable  $\text{Na}^+$  intercalation/deintercalation and huge volume expansion.<sup>3</sup> In order to achieve extremely high capacity, Li-S batteries are even more promising because the cathode is made of sulfur which is abundant, and has high theoretical capacitance ( $1675 \text{ mA h g}^{-1}$ ), and high specific energy ( $\sim 2600 \text{ W h kg}^{-1}$ ). However, the Li-S batteries suffer from low sulfur loading, interfacial instability of lithium-metal anodes, shuttling of lithium polysulfides and sluggish kinetics of  $\text{Li}_2\text{S}$  activation, which hinder their commercial application. Among metal-air batteries, rechargeable ZABs get attention due to their high theoretical energy density ( $1086 \text{ W h kg}^{-1}$ ), excellent safety (aqueous electrolyte), unique open structure and abundance of zinc in earth's crust, consuming atmospheric oxygen as a cathodic active material.<sup>4</sup> However, ZABs currently suffer from poor cycling stability and inferior charging/discharging rates. Another interesting idea for aeronautics and automotive sectors is the use of structural batteries, *i.e.* carbon-fiber (CF) composites which combine two functions in one device; they not only act as structural components but also as batteries to enable distributed energy storage in an airplane or a car, allowing reduction in complexity and weight.<sup>5,6</sup> The major issues associated with structural batteries are poor mechanical performance of the cathode electrodes and low energy density due to the CF-based electrodes. In general, all types of batteries suffer from low power density due to the sluggish redox reactions/intercalation of the electrode material. Hybrid SCs, also called hybrid energy storage devices, based on a combination of electrostatic and electrochemical storage were also developed to combine the advantages of batteries and SCs.<sup>7</sup> However, hybrid SCs show relatively lower specific power density compared to the conventional capacitors and also lower energy densities than typical batteries.

To address the issues associated with these energy storage technologies, the most efficient strategy is to develop appropriate electrode materials, understand the electrochemical mechanism behind them and modify the properties and structure of the electrode materials by different manufacturing and synthesis processes.

Although different energy storage technologies show different energy storage mechanisms, their electrochemical performance always depends, with no exception, on the structure and properties of electrode materials.<sup>8</sup> As an example, the ionic conductivity of electrode materials determines the power density of a device; the charge/discharge rate depends on the electric conductivity of electrode materials; low surface areas of electrode materials result in inferior energy density; the poor mechanical properties of

electrode materials lead to poor stability of the energy storage devices.

Two-dimensional nanosheets like graphene and graphene-related materials (termed GRMs hereafter) are ideal for energy storage, having a combination of structural/compositional properties which allow solving the abovementioned issues; for example, excellent electrical conductivity, high mechanical properties, large specific surface areas, rich surface chemistry and flexibility in the structure. The unique 2D structure and properties of GRMs make them promising electrode materials for batteries and SCs, as they can result in fast electron transport, fast ion diffusion and excellent ion storage ability, boosting electrochemical energy storage performances.

In this feature article, we first summarize the general challenges affecting energy storage devices including poor electric conductivity, sluggish ion diffusion, low surface areas, poor mechanical properties, self-discharge and limited cell configurations. To overcome these issues and improve the performance of energy storage technologies, we then discuss the strategies that we have developed in recent works with a focus on structure manipulation and surface modification of graphene. Lastly, we provide the outlook and perspective on the use of GRMs to understand the mechanism of energy storage and further improve the performance of energy storage devices.

## 2. Challenges to improve electrode materials in batteries and SCs

This section provides a schematic summary of the challenges associated with electrode materials in batteries and SCs.

### Challenge 1: low ionic conductivity

The first general challenge faced in batteries and SCs is to increase the ionic conductivity of electrode materials, because it plays an important role in the rate performance and overall energy density (Fig. 1(a)).<sup>9</sup> As an example, pseudocapacitive oxides exhibit good energy storage performance but low intrinsic ionic conductivity, causing high electrode resistance. Layered materials can store energy thanks to the ion intercalation mechanism, but the long ion diffusion pathway lowers the ionic conductivity and deteriorates the rate performance.

### Challenge 2: low electrical conductivity

Low electrical conductivity is another problem leading to inferior electrochemical performance of batteries and SCs due to sluggish electron transport in electrode materials (Fig. 1(b)). The improvement in ionic conductivity and electric conductivity leads to fast ion and electron accumulation on the surface of electrode materials, which results in high-rate performance at high current density.

### Challenge 3: low specific surface area

The state-of-the-art electrodes in batteries and SCs also face problems of a low specific surface area (Fig. 1(c)). The limitation of an ion-accessible surface area in pristine electrode materials





Fig. 1 Challenges of electrode materials in batteries and SCs schematized from the literature. (a) Low ionic conductivity. Reproduced with permission.<sup>9</sup> Copyright 2020, Elsevier. (b) Low electronic conductivity. (c) Low specific surface area. (d) Poor mechanical properties. (e) Self-discharge. Reproduced with permission.<sup>11</sup> Copyright 2020, American Chemical Society. (f) Limited cell configuration. Reproduced with permission.<sup>13</sup> Copyright 2021, Wiley-VCH Verlag GmbH & Co. KGaA, Weinheim.

greatly inhibits the accumulation of ions on the surface, and restrains the chemistry reaction and the formation of EDLs in the electrodes, having a significant influence on the final capacity of batteries and capacitance of SCs. In contrast, a large specific surface area allows storage of a large number of ions and faster access to the electrolyte inside the nanomaterials, which effectively reduces the ion diffusion distance.<sup>10</sup>

#### Challenge 4: poor mechanical and electrochemical stability

The poor mechanical stability of electrode materials is a limiting factor for the development of stable batteries and SCs (Fig. 1(d)). The first issue which causes the poor stability is the electrode expansion and contraction attributed to reversible intercalation of ions. Volume changes may result in cracking and exfoliation of the electrode material from the current collector during the charge/discharge process. Even if the material does not detach completely from the electrode, the fracture causes a decay in capacity and poor cycling stability. Improving the mechanical properties of electrode materials is a key challenge in particular in developing flexible devices.

#### Challenge 5: self-discharge

Open circuit self-discharge, caused by the diffusive properties of the soluble species in the electrolyte and unstable electrostatic interactions (Fig. 1(e)), is a big issue associated with batteries and SCs.<sup>11</sup> In general, the self-discharge phenomenon is caused by the following four factors: (1) parasitic currents at one or both electrodes, (2) charge release across the double layer due to overcharged cells, (3) ohmic leakage between

two electrodes, and (4) charge redistribution caused by non-homogeneous charging,<sup>12</sup> due to different accessibility for the ions to different parts of the electrode, causing diffusion controlled leakage.<sup>12</sup> In particular for batteries, the shuttle effects of soluble redox species in the electrolyte can give rapid self-discharge.

#### Challenge 6: limited cell configurations

The common configuration of batteries and SCs contains two electrodes separated by a separator.<sup>13</sup> Various multifunctional batteries and SCs need to be developed to satisfy the potential applications in wearable and portable electronics. Also due to the miniaturization of electronic instruments, a smaller size of batteries and SCs is needed.

## 3. Advantages of using GRMs in energy storage materials

Graphene is a single-atom-thick 2D crystalline material consisting of only carbon atoms, arranged in a hexagonal lattice. It is the first discovered, most popular and, currently, the cheapest and most abundant member of the large family of 2-dimensional materials. Due to its excellent intrinsic properties, graphene shows great potential for various energy storage related applications (Fig. 2).

Graphite is already a very good material to store ions; the possibility to exfoliate graphite in graphene sheets, functionalize them and then reassemble them in less compact structures gives fantastic opportunities to create GRM shaped as 3-dimensional structures composed of 2-dimensional nanosheets. These macro/mesoporous structures allow easy access to electrolyte ions, meanwhile maintaining excellent electrical conductivity and good mechanical properties of the electrodes.<sup>14</sup> Down to nano- and angstrom-scale, the slit-shaped channels formed by the assembling of functionalized nanosheets provide a 2D-confined space for efficient intercalation of specific ions. For example, functionalized graphene with enlarged interlayer distance and modified surface chemistry allows the intercalation of sodium, which is not possible with conventional graphite, thus fostering the development of cheap SIBs.<sup>15</sup> Due to the excellent structures of GRM, these materials can be used for a large range of electrochemical energy storage applications such as lithium ion batteries, sodium ion batteries, Li-S batteries, rechargeable ZABs, structural batteries and hybrid SCs.

In the following sections, we will describe different structures which use GRM for improving electrode materials.

## 4. Composite structures obtained by functionalization and stacking of graphene-related materials

### 4.1. Graphene-related materials to enhance ionic conductivity

Graphene sheets can be modified and stacked in composite structures, creating slit-shaped channels with a spacing larger than that naturally present in graphite, and by chemically





Fig. 2 Some typical structures and applications of graphene-related materials.

functionalizing to enhance ion diffusion and storage. In this section, we describe four different strategies that we demonstrated in recent years to achieve this goal.

**4.1.1. Tuning of the interlayer distance.** The interlayer distance in graphite is  $d = 0.34$  nm, not enough for intercalation of large ions. Conversely, in graphene stacks  $d$  can be tuned by the intercalation of exotic species, *e.g.*, functional groups, solvent molecules, organic molecules or even polymers.<sup>16–22</sup> Interlayer distance in graphene oxide (GO), could reach  $d > 0.75$  nm due to the presence of oxygen containing functional groups and further be increased to  $d > 2$  nm after the intercalation of water or solvents. Such enlarged interlayer distance and hydrophilic surface properties allow the intercalation of large-sized solvated ions. As an example, we recently described how solvated tetraethylammonium ions (TEA) and acetonitrile intercalate in Brodie graphite oxide (BGO), creating complex stacked structures in which spacing can vary with temperature and TEA concentration (Fig. 3(a)).<sup>23</sup> At low TEA concentration, only acetonitrile intercalates in BGO nanosheets, forming one or two intercalated layers, with  $d \approx 8.9$  Å and  $d \approx 12.5$  Å, respectively. The larger TEA ions do not penetrate into either of the structures. At high TEA concentrations, instead, temperature-dependent TEA intercalation is observed, forming a new phase with a distinct interlayer distance of  $d \approx 15$ – $16.6$  Å, with a clear phase transition at 0 °C. The electrochemical capacitance of the material benefits from this complex behaviour, with capacitance transition observed at different temperatures and concentrations; Fig. 3(b) shows a sharp change in the capacitance slope when the solvated electrolyte ions are inserted into the slit pores of the BGO structure.

Large molecules can be included in the layered structures also during the synthesis. For example, we designed and synthesized another complex intercalated spacer, *i.e.*, 3D rigid tetrakis(4-aminophenyl)methane (TKAm) molecules, and

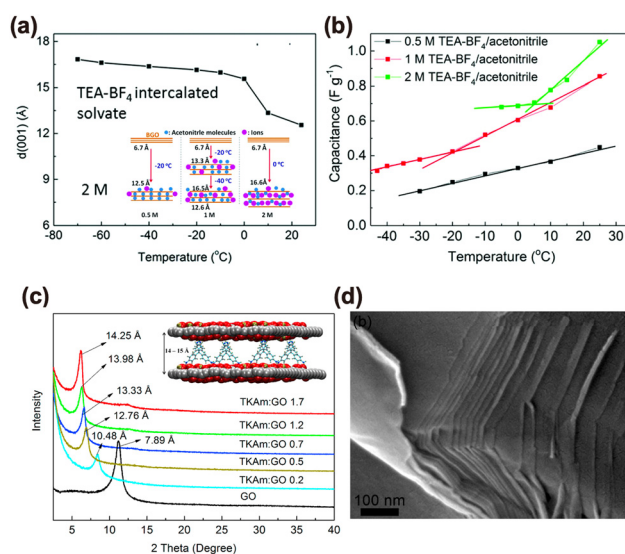


Fig. 3 Examples of GRMs used to boost the ionic conductivity of electrode materials. (a) Temperature dependence of the (001)  $d$ -spacing for BGO in 2 M TEA-BF<sub>4</sub> electrolyte. The inset shows a scheme of the interlayer spacing adjustment *via* temperature- and concentration-dependent intercalation of solvated TEA-BF<sub>4</sub> ions into BGO. (b) Comparison of the specific capacitances of BGO electrodes in 0.5, 1, and 2 M TEA-BF<sub>4</sub>/acetonitrile under various temperatures. Reproduced with permission.<sup>23</sup> Copyright 2018, Royal Society of Chemistry. (c) XRD patterns of the samples with various loading of TKAm:GO. The inset shows a schematic illustration of the pillared GO/TKAm structure. (d) SEM image of the H-GO/TKAm sample grain edges. Reproduced with permission.<sup>24</sup> Copyright 2017, Elsevier.

intercalated them into GO layers with the formation of stable 3D porous pillared GO frameworks.<sup>24</sup> Due to the presence of pillaring molecules between the GO sheets, the interlayer spacing could be tuned from 7.89 to 14.25 Å by intercalating different amounts of TKAm molecules (Fig. 3(c)



and (d)) reaching a specific surface area (SSA) of up to  $660 \text{ m}^2 \text{ g}^{-1}$ , which is among the highest reported values for GO materials pillared with organic spacers.

One of the benefits of enlarged interlayer distance is to allow barrier-free intercalation of ions and fast diffusion of ions between the graphene layers, resulting in high ionic conductivity and storage capacity. In a recent study, we used functionalised graphene to understand how sodium ions can be stored to develop high performance SIBs.<sup>15</sup> We addressed the scientific question of why sodium ions cannot effectively intercalate into graphite while lithium ions, just above sodium in the periodic table, can. We designed and synthesized graphene with aminobenzene (AB) asymmetric functionalization, termed “Janus” graphene (Fig. 4(a)–(c)), which allowed the reversible intercalation of sodium ions. The mechanism of sodium ion storage was rationalized using density functional theory (DFT) calculations, showing that the aminobenzene molecules not only act as spacers, but also create additional active sites for the storage of  $\text{Na}^+$  (Fig. 4(d)). We monitored this process in real

time by operando Raman spectroscopy and electro-chemical measurements (Fig. 4(e)). During intercalation, the G band shifted from  $1595$  to  $1605 \text{ cm}^{-1}$  at a discharge potential of approximately  $0.6 \text{ V}$  versus  $\text{Na}^+/\text{Na}$ , confirming the positive doping of  $\text{Na}^+$  in graphene. We used, for the first time, ellipsometry imaging to visualize in real space and real time the intercalation and fast diffusion of sodium ions from the edges of the Janus graphene stacks to the center (Fig. 4(f) and (g)). Noteworthy, the significant binding energy of sodium ions with the spacer does not hinder  $\text{Na}^+$  diffusion between the graphene sheets. Asymmetric functionalization with the formation of Janus structures provides a novel strategy to modify graphite in order to use this cheap and abundant carbon material for high-performance sodium ion batteries.

**4.1.2. Fabrication of nanometer-sized pores.** A second strategy, different from the use of spacers, is the creation of nanometer-sized pores on the surface of graphene, to increase the ionic conductivity. In this way, instead of going through the 2D tortuous channels, ions can drift directly through pores in



Fig. 4 (a) Scheme of the preparation of the stacked Janus graphene thin film. (b) Cartoon showing the intercalation of  $\text{Na}^+$  ions in the interlayer space of Janus graphene sheets. (c) Optical microscopy of AB graphene multilayers. (d) Isosurface of differential charge density calculated in the presence of  $\text{Na}^+$ . (e)–(g) Observation of  $\text{Na}^+$  intercalation/deintercalation in real time with different techniques: (e) Raman spectroscopy, (f) imaging ellipsometry of angle  $\Delta$ , and (g) current–time profile. Reproduced with permission.<sup>15</sup> Copyright 2021, American Association for the Advancement of Science.



the graphene layers. Chemical etching is an efficient and controllable way to introduce nanometer-sized pores on the surface of GO (Fig. 5(a)).<sup>25</sup> The nanopores on GO sheets can be observed by high-resolution transmission electron microscopy (HR-TEM) (Fig. 5(b)). After the reduction process, the oxygen containing functional groups can be removed, but the nanometer-sized pores are preserved. Thus, this electrode material could satisfy both requirements of having high electrical conductivity and porous structures for electrochemical energy storage.

**4.1.3. Fabrication of a 3D porous structure.** A third strategy to increase ionic conductivity is the fabrication of a 3D porous structure. The formation of a hierarchical structure including 1D nanometer-sized micropores on the graphene surface, the 2D nanometer sized porous channels, and further 3D macropores can maximize the ionic diffusion and achieve ideal ionic conductivity. To this aim, we prepared a 3D porous composite structure made of fluorine-doped SnO<sub>2</sub> and reduced graphene oxide (F-SnO<sub>2</sub>@RGO) as an anode material for LIBs.<sup>26</sup> The 3D porous structure was formed during the hydrothermal process by the self-assembling of RGO nanosheets, while the F-SnO<sub>2</sub> nanoparticles were uniformly decorated on the surface of the 2D sheets (Fig. 5(c)). The pores formed could accommodate the electrolyte and allow the fast diffusion of ions, leading to high ionic conductivity. As an anode for lithium-ion batteries, the F-SnO<sub>2</sub>@RGO composite showed excellent rate performance and cycling stability (Fig. 5(d)) due to the fast lithium-ion diffusion (Li ion diffusion coefficient  $D_{\text{Li}} = 9.87 \times 10^{-17} \text{ cm}^2 \text{ s}^{-1}$ ) and high electrical conductivity.

**4.1.4. Assembly of vertically aligned nanosheets.** The construction of nanosheets vertically aligned on a conductive electrode substrate is another strategy to offer fast ion diffusion routes from electrolyte to electrodes. The vertically aligned

nanosheets enhance ionic conductivity, the ion transference number, mechanical strength, and electrochemical performance. We created vertical structures of microporous covalent organic framework (*i.e.*, COF-1) nanosheets on the surface of GO using benzene-1,4-diboric acid (DBA) as molecular pillars (Fig. 6(a)).<sup>27</sup> The SEM image showed that the COF-1 nanosheets were vertically anchored on the surface of GO (Fig. 6(b)). After the conversion, an all-carbon material with vertical porous carbon nanosheets on RGO (v-CNS-RGO) was obtained. The electrochemical performance of the composites was evaluated and the cyclic voltammetry (CV) curves of v-CNS-RGO electrodes presented quasi-rectangular shape at various scan rates, indicating the typical capacitive behaviour. A large hump observed in the CV curve was attributed to the pseudocapacitance of B-doped carbon nanosheets (Fig. 6(c)). We demonstrated the importance of the alignment of the structures by comparing the capacitance of electrodes having vertical or horizontal nanosheets on the substrate (Fig. 6(d)), with the former providing better capacitance due to the better ionic and electric conductivity.

## 4.2. Graphene-related materials to boost electric conductivity

The low electric conductivity of electrode materials is another limitation that inhibits the fabrication of high-performance batteries and SCs.<sup>28</sup> Applications in electric vehicles, in particular, require batteries and SCs with both high power density and high energy density, which need electrode materials with high electric conductivity. GRMs, having high conductivity and large aspect ratios, are an ideal additive in composite materials to improve electric conductivity and electrochemical performance.

The presence of graphene nanosheets dispersed on a nanoscale in a composite could provide conductive networks for improving the electrical conductivity of electrodes. Using graphene as a conductive support and a template for the nucleation of Ni-Al layered double hydroxide (LDH), we prepared graphene/Ni-Al LDH nanowires using a simple hydrothermal



**Fig. 5** (a) Schematic models of porous GO. (b) An HR-TEM image of GO sheets. Reproduced with permission.<sup>25</sup> Copyright 2019, Springer Nature. (c) SEM image of F-SnO<sub>2</sub>@RGO composite. (d) Cycling stabilities of the F-SnO<sub>2</sub>@RGO and SnO<sub>2</sub>@RGO electrodes and the corresponding Coulombic efficiency. Reproduced with permission.<sup>26</sup> Copyright 2015, American Chemical Society.



**Fig. 6** (a) Scheme of vertically aligned structure of COF-1 nanosheets using DBA as molecular nucleation sites. (b) SEM image of v-COF-GO nanocomposite. (c) CV results of the v-CNS-RGO composites. (d) Capacitance comparison of vertically (v-CNS-RGO-3) and horizontally (CNP/RGO-3) grown nanosheets on GO. Reproduced with permission.<sup>27</sup> Copyright 2018, Wiley-VCH Verlag GmbH & Co. KGaA, Weinheim.



process (Fig. 7(a)).<sup>29</sup> The presence of graphene boosted the electrical conductivity of the resulting graphene/Ni–Al LDH composites, resulting in an improved electrochemical performance.<sup>30</sup> The rectangular shape of the CV loops confirmed the ideal capacitive behaviour (Fig. 7(b)). Electrochemical impedance spectroscopy (EIS) measurements demonstrated that the graphene/Ni–Al LDH nanowires possessed the lowest charge transfer resistance ( $R_{ct} = 3.4 \Omega$ ) (Fig. 7(c)). The vertical line at low frequencies indicated the ideal capacitive behaviour and low diffusion resistance of ions.

RGO can be used in electrode materials not only to enhance conductivity but also as a substrate and protective layer, as described in the following examples. RGO does not possess the excellent conductivity of graphene, and one could argue thus that is not the best additive to boost electric conductivity; however, RGO can reach, if properly reduced, conductivities higher than typical conductive polymers, and much higher than the typical energy storage materials. We studied the mechanism of charge transport in RGO by tuning independently the sheet size, temperature and number of layers.<sup>31</sup> We demonstrated in this way that charge transport in RGO proceeds through variable range hopping (VRH) according to the Efros–Shklovskii model below a critical temperature  $T^*$ , and a power-law behaviour is observed above this temperature.

Charge transport does not depend much on the size of the nanosheets but primarily on charge localization length  $\xi$ , which is the size of overlapping  $sp^2$  domains belonging to different nanosheets; the electrical behaviour of the network is dominated by the inter-sheet transport through such overlapping aromatic regions. In this way, RGO sheet conductivity can range from  $10 \text{ S m}^{-1}$  to  $10^5 \text{ S m}^{-1}$ , good enough for applications in electrodes.

### 4.3. GRMs to improve the specific surface area

The large specific surface area of electrode materials provides abundant exposed active sites for ion storage and alleviates the mechanical stress induced by volume swelling during charge/discharge cycles. Also, in this case graphene has ideal properties with a large specific surface area of  $2630 \text{ m}^2 \text{ g}^{-1}$  (theoretical value). However, in real materials, GRM nanosheets tend to restack and aggregate. The assembly of 2D nanosheets in 3D structures is an efficient method to mitigate the aggregation

issue, thus providing abundant inner space for ion storage. To achieve this aim, we prepared highly conductive 3D macroporous RGO thin films (MGTFs) using ice crystal-induced phase separation followed by thermal or chemical reduction processes.<sup>32</sup> The thickness of MGTF hierarchical porous thin films could be controlled from hundred nanometers to tens of micrometers, with thickness influencing the inner structure of the MGTFs formed by an open, interconnected macropore structure (Fig. 8(a)). The hydrophilic surface of MGTFs promoted efficient wetting of the MGTFs in an aqueous solution and accelerated electrolyte diffusion inside the MGTFs. MGTFs functionalised with CdSe nanocrystals were used as photoactive electrodes for photoelectrochemical  $\text{H}_2$  generation (Fig. 8(b)); the uniform deposition of CdSe nanoparticles in the network allowed prevention of recombination of generated electron-hole pairs beyond the intrinsic diffusion length.

More complex, multilayer GRM composites structures could be assembled using a two-step electrochemical approach combining electrophoretic deposition (EPD) and cathodic electro-deposition (CED). In this way, we fabricated multilayer hierarchical electrodes of RGO and mixed transition metal sulfides ( $\text{NiCoMnS}_x$ ) directly on 3D graphene foam (GF) substrates.<sup>33</sup> In the composite stack, RGO interlayer coatings favoured a uniform distribution of  $\text{NiCoMnS}_x$  nanosheets (Fig. 8(c) and (d)). This material with a large surface area and multilayer structure showed high performance activity as an electrode for cathodes in rechargeable alkaline batteries (RABs). The Ragone plot showed a high specific energy of  $97.2 \text{ W h kg}^{-1}$  at a specific power density of  $108 \text{ W kg}^{-1}$ . The corresponding RAB showed a high specific power density of  $3.1 \text{ kW kg}^{-1}$  at a specific energy density of  $44 \text{ W h kg}^{-1}$ . The excellent rate performance of the RAB (Fig. 8(e)) was attributed to RGO layers acting as porous spacers to increase electrical conductivity and protect sulfides against delamination and agglomeration.

### 4.4. Graphene-related materials to improve the mechanical properties and integration of the electrochemical devices

Mechanochemical degradation processes of electrode materials severely deteriorate the cycling life of batteries and SCs.<sup>34</sup> Graphene has excellent mechanical properties, with a Young's modulus of  $\sim 1 \text{ TPa}$  ( $\sim 340 \text{ N m}^{-1}$ ) and a breaking strength of



Fig. 7 GRMs to improve electrical conductivity. (a) SEM image of graphene supported Ni–Al LDH sheets. (b) CV curves of the graphene/Ni–Al LDH nanowires at various scan rates. (c) EIS results of various LDH materials and RGO. Reproduced with permission.<sup>29</sup> Copyright 2014, Royal Society of Chemistry.





**Fig. 8** GRM to improve the specific surface area of electrodes. (a) SEM image of macroporous RGO. (b) Schematic structures of photoelectrochemical  $H_2$  generation for CdSe@MGTF and CdSe@CGTF electrodes. Reproduced with permission.<sup>32</sup> Copyright 2015, Wiley-VCH Verlag GmbH & Co. KGaA, Weinheim. (c) Scheme of multilayer RGO-NiCoMn $S_x$  architectures and (d) corresponding SEM image, with artificial colours to show the different phases in the layers. (e) Ragone plot of the devices using NCMS at various current densities. Reproduced with permission.<sup>33</sup> Copyright 2022, Wiley-VCH Verlag GmbH & Co. KGaA, Weinheim.

$\sim 125$  GPa ( $\sim 42$  N m $^{-1}$ ) and is thus an ideal additive to be used in flexible electronics and in structural batteries.<sup>35,36</sup>

We previously mentioned how to assemble macroporous RGO thin films (MGTF) on rigid substrates using ice-crystal-induced phase separation;<sup>32</sup> we used the same approach to assemble MGTFs on flexible graphene papers (GPs), to fabricate flexible, high-performance SCs.<sup>37</sup> The macroporous structure provided an accessible large surface area and a porous surface for the electrochemical deposition of conductive polyaniline (PAN) nanofibers (Fig. 9(a)–(c)). We obtained a PAN@MGTF@GPs composite which inherited the porous nature of MGTFs, and

was mechanically stable even under 90° bending. The strength and flexibility of the composite ensured high performance of flexible SCs, demonstrated by CV tests performed before and after rolling (Fig. 9(d)).

Micro-supercapacitors (MSCs) are miniaturized SCs that are small enough to be integrated into electronic devices.<sup>38</sup> They can be integrated either as self-powering systems with charging through energy harvesters, or enhanced microbattery systems where they act as hybrid devices with batteries to improve the lifetime of a device. MSC design is based on the same considerations as SC-electrodes with additional requirement of



**Fig. 9** GRMs to improve the mechanical properties of the electrodes. (a) Optical photograph of flexible MGTF@GPs. SEM images of MGTFs at (b) low magnification and (c) high magnification. (d) CV curves of the flexible PAN@MGTF@GP composite electrode under different bending. Reproduced with permission.<sup>37</sup> Copyright 2016, American Chemical Society. (e) Schematic illustration of the inkjet-printed graphene MSCs. (f) CV curves of MSCs at various scan rates. (g) GCD results of the Fe–Mn based MSC. Reproduced with permission.<sup>38</sup> Copyright 2021, Royal Society of Chemistry.



high mechanical stability.<sup>39</sup> With such consideration, we integrated graphene with fragile metal oxides to improve their electrochemical stability, flexibility and mechanical properties. The inks prepared in this way showed high colloidal stability, suitable for inkjet printing of MSCs. Conductive exfoliated graphene (EG) inks were printed on a Kapton substrate to fabricate planar interdigitated micropatterns (Fig. 9(e)).<sup>38</sup> Taking advantage of the conductivity of EG, MnO<sub>x</sub> or FeOOH nanoflakes could be electrodeposited on the EG pattern using pulse current deposition. Fe<sub>2</sub>O<sub>3</sub> or MnO<sub>2</sub> was finally obtained by annealing at 300 °C. These MSCs showed excellent rate performance, a high stack capacitance of 110.6 F cm<sup>-3</sup> measured from galvanostatic charge–discharge (GCD) at a current density of 5 μA cm<sup>-2</sup> (Fig. 9(g)) and high cycling stability (95.7% capacitance retain) after 10 000 cycles.

We used similar electrodeposition methods also on a larger scale, to assemble structural batteries. These are particular devices for applications in aeronautics or automotive, where the carbon fibers (CF) forming the structure of the vehicle can be modified to store energy, acting as distributed batteries as well.

In structural batteries, one layer of CFs acts as an anode, and another layer acts as a cathode, with a porous polymer matrix containing the electrolyte in between. Structural batteries usually suffer from low-capacity retention due to the poor mechanical performance of the cathode electrodes. Recently, we showed a significant improvement in the cathode performance by adding electrochemically exfoliated graphene oxide (EGO) on its surface *via* the EPD process, as seen in the schematic diagram in Fig. 10(a).<sup>6</sup> We tested full cells having a pristine CF negative electrode and a LiFePO<sub>4</sub>/EGO coated CF cathode in liquid electrolyte. They achieved a maximum

specific capacity of 79.85 mA h g<sup>-1</sup> with 88.1% capacity retention at 1 C after 300 cycles (Fig. 10(b) and (c)). This excellent cycling behaviour is attributed to efficient charge transfer and a favourable mass balance between electrodes, with a uniform, mechanically stable and continuous conductive network of LiFePO<sub>4</sub>/EGO formed on the electrodes.

#### 4.5. Modification of surface chemistry of graphene-related materials to address the above challenges

The modification of surface chemistry of electrode materials plays a critical role in hindering gas evolution in lithium ion batteries,<sup>40</sup> enhancing the stability of lithium–air batteries,<sup>41</sup> improving electron conductivity of electrode materials of SIBs,<sup>42</sup> increasing the wettability of electrodes, and increasing the electrode kinetics of SCs.<sup>43</sup> Introducing specific surface functional moieties on the graphene surface is an important strategy to control its electrochemical activity and improve its electrochemical performance. Graphene is chemically stable, so specific strategies should be used for its functionalization.

##### 4.5.1 Surface doping of graphene-related materials.

Heteroatom doping is a popular strategy to construct highly active bifunctional electrocatalyst materials for oxygen reduction reaction (ORR) and oxygen evolution reaction (OER) in ZAB applications. Doping graphene with heteroatoms such as nitrogen or anchoring transition metals on the surface generates more active sites, which leads to the enhancement of the electrocatalytic activity of the material. With this aim, we developed nitrogen-doped RGO (N-RGO) functionalised with non-precious metal nanoparticles. The coupling between non-precious metal particles and N-RGO has a synergistic effect which improves the oxygen electrochemistry of the composite material. Following this strategy, we anchored quaternary spinelsulfide (NiCoMnS<sub>4</sub>) nanoparticles on the surface of N-RGO layers to fabricate NiCoMnS<sub>4</sub>/N-RGO hybrids *via* a hydrothermal method (Fig. 11(a)).<sup>44</sup> The NiCoMnS<sub>4</sub>/N-RGO hybrid could be used as an air-cathode for Zn–air batteries reaching a peak power density of 56 mW cm<sup>-2</sup> (93 W g<sub>catalyst</sub><sup>-1</sup>) at 79 mA cm<sup>-2</sup>. In addition, metal oxide nanorods (NRs) were also hybridized with N-RGO to fabricate a highly efficient bifunctional electrocatalyst (Fig. 11(c)).<sup>45</sup> The ZABs based on this hybrid material showed larger specific capacity than the batteries using the commercial PtRuC 20% catalyst at 5 mA cm<sup>-2</sup> (Fig. 11(d)), thanks also to the contribution of nitrogen-doped RGO in the ORR.

##### 4.5.2 Surface functionalization of graphene-related materials.

Grafting organic molecules is one of the most popular strategies to modify the surface chemistry of graphene, but usually the grafting position is random. We developed a two-step process combining supramolecular chemistry and electrochemistry to graft ordered patterns of molecules on graphene.<sup>46</sup> The process has two independent steps: (1) self-assembly into an ordered array of molecules on graphene from an organic solvent, thanks to supramolecular, noncovalent interactions (Fig. 12(a) and (b)). The sample is then transferred into an aqueous electrolyte, to block any reorganization or desorption of the monolayer. Then, (2) an electrochemical impulse is used to transform a diazonium group of the molecule into a radical capable of grafting covalently to the substrate,

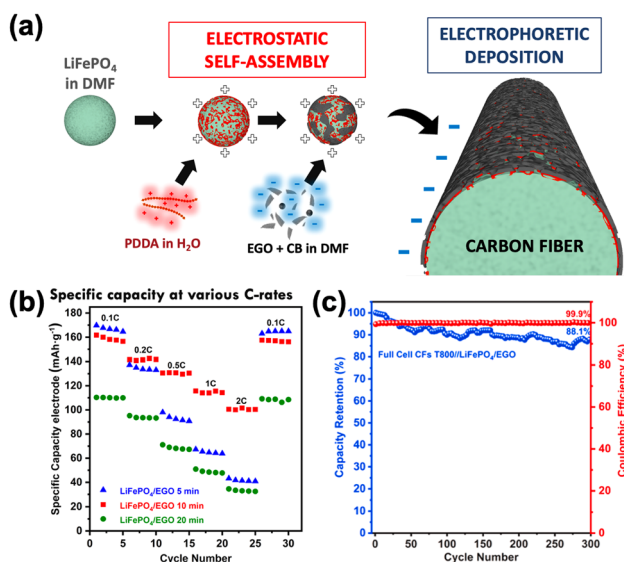


Fig. 10 (a) Schematic illustration of EPD synthesis of the LiFePO<sub>4</sub>/EGO electrode composite. (b) Specific capacities (normalized over the total mass of both electrodes, anode and cathode) at various C-rates. (c) Cycling performance and Coulombic efficiency at 1C. Reproduced with permission.<sup>6</sup> Copyright 2021, Elsevier.





**Fig. 11** (a) TEM image of the NiCoMnS<sub>4</sub>/N-RGO hybrid. (b) Galvanodynamic discharge profile and power density of NiCoMnS<sub>4</sub>/N-RGO air cathodes. Reproduced with permission.<sup>44</sup> Copyright 2019, Elsevier. (c) TEM image of N-RGO/Co<sub>3</sub>O<sub>4</sub> NRs nanohybrid. (d) The comparison of discharge profiles of ZABs with N-RGO/Co<sub>3</sub>O<sub>4</sub> NRs and commercial PtRuC 20% as oxygen electrode catalysts. Reproduced with permission.<sup>45</sup> Copyright 2020, Royal Society of Chemistry.

thus transforming the physisorption into covalent chemisorption. During grafting, the molecules retain the ordered packing formed upon self-assembly. Our two-step approach features an independent control over the processes of immobilization of molecules on the substrate and their covalent tethering, enabling fast ( $t < 10$  s) covalent functionalization of graphene. This strategy is highly versatile and can be used on many different substrates, *e.g.*, graphene deposited on silicon, plastic, and quartz as well as highly oriented pyrolytic graphite.

We used a similar approach, based on diazonium chemistry, also to functionalise the Janus graphene already described in Section 4.1. The aminobenzene spacers, besides increasing inter-sheet spacing, also stabilize the physisorption of the Na<sup>+</sup> ions through electrostatic interactions, as demonstrated by experiments and DFT (Fig. 4(b) and (d)). Functionalized graphene can also be used to address the well-known issue of the shuttle effect in Li-S batteries, caused by the migration of



**Fig. 13** Surface modification of GRM to improve ion storage. (a) Schematic illustration of the fabrication of NG and SG by diazonium chemistry. (b) Cycling stability of the SG hosts. (c) Optimized structures corresponding to the strength of interactions. Reproduced with permission.<sup>47</sup> Copyright 2021, Wiley-VCH Verlag GmbH & Co. KGaA, Weinheim.

soluble polysulfides which diffuse from the cathode to the anode, causing a rapid decrease in the capacity and poor Coulombic efficiency during charge/discharge cycles. To achieve this aim, we functionalized expanded reduced graphene oxide (eRGO) in order to increase the interaction of its surface with soluble lithium polysulfides. We prepared eRGO functionalized with nitrobenzene (NG) and benzene sulfonate (SG) by grafting 4-nitrobenzene diazonium tetrafluoroborate and 4-sulfonic acid phenyl diazonium tetrafluoroborate on the surface of eRGO, respectively (Fig. 13(a)).<sup>47</sup> We also prepared Li/S cells made using SG, which showed high cycling stability (Fig. 13(b)); this was due to the strong interaction between sulfonate functional groups and polar lithium polysulfides, which inhibited the shuttle effect of Li-S batteries, as confirmed also by DFT simulations used to model the interaction of sulfur and LiPs with the SG groups (Fig. 13(c)).

## 5. Conclusions

In this feature article, we described the different approaches that we used to exploit the unique properties and high processability of graphene to assemble new materials for energy storage.

We first summarized the general challenges associated with both batteries and SCs, including poor ionic conductivity, low electric conductivity, low specific surface areas, poor mechanical and electrochemical stability, self-discharge and limited cell configurations. Various strategies were proposed and discussed with the purpose to understand and address those challenges by integrating graphene-related materials into the electrode materials as either active materials or conductive additives. The regulation of interlayer spacing of graphene, formation of hierarchical 3D graphene structures, porous GO sheets and vertically aligned composites are effective strategies summarized in this feature article. In particular, oriented

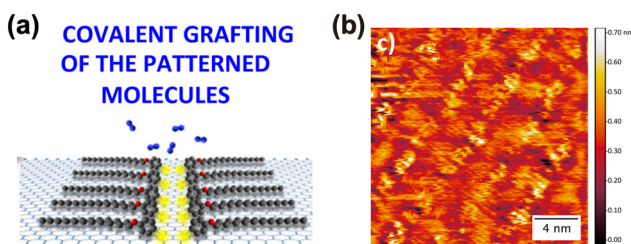


**Fig. 12** (a) Scheme of the covalent grafting of patterned molecules on the surface of graphene. (b) STM height image of molecules self-assembled on graphene. Reproduced with permission.<sup>46</sup> Copyright 2016, American Chemical Society.



graphene with stable pillars in between offers ionic transport channels, which are beneficial to the improvement of ionic conductivity.<sup>48</sup> Films composed of stacked GRM porous nanosheets increase the ion diffusion not only along the nanosheets, but also across the pores. Graphene with high mechanical strength is used to assemble the wearable electronics and electronic skin, for example, for the flexible SCs. In addition, the MSCs are assembled using the graphene-related materials to obtain high electrochemical performance.

The modification of surface chemistry of graphene is another efficient strategy to regulate the electrochemical performance. Using graphene-related materials in electrodes could dramatically increase the ionic conductivity, electron transport, and specific surface area.<sup>49,50</sup> The modification of surface chemistry of graphene offers the novel methods for the fabrication of high-performance SIBs and Li-S batteries. The self-discharge phenomenon and limited cell configurations are still remaining issues to be solved.

## 6. Outlook and perspective

Although great achievements have been accomplished, the advanced material design based on graphene still needs long-term development. In the future, further developments of batteries and SCs based on graphene-related materials need to be carried out in the following two directions: (i) constructing novel hierarchical structures of graphene-based composite materials. The unique structure endows graphene with excellent properties, such as high mechanical strength for application in flexible devices. It may provide promising applications including human motion monitoring and flexional mobile electronics.<sup>51</sup> (ii) Modification of the surface chemistry of graphene-related materials with highly redox active molecules to boost the electrochemical performance of various energy storage devices. Nowadays, both high specific power density and energy density are important for the practical application of energy storage devices, especially due to the rapid popularization of electric vehicles which suffer from a limited travel distance and long recharge time.

In conclusion, we are convinced that the versatile electronic, chemical and mechanical properties of GRMs can be used even better to develop novel composite architectures allowing the invention of a new generation of batteries and SCs. The rational modification of graphene is a beacon of hope for boosting the specific power density and energy density of such devices simultaneously.

## Conflicts of interest

There are no conflicts to declare.

## Acknowledgements

The authors acknowledge the support from the European Union's Horizon 2020 research and innovation program in GrapheneCore3 881603-Graphene Flagship (Spearhead 3 project and WP14),

the Swedish Research Council in project Janus 2017-04456, the FLAG-ERA project (2019-03411 and 2021-05924), the ÅForsk young researcher project (21-393), the National Natural Science Foundation of China (22205071), and the University Natural Science Research Project of Anhui Province (KJ2021A0523).

## References

- 1 R. Rojaee and R. Shahbazian-Yassar, *ACS Nano*, 2020, **14**, 2628–2658.
- 2 M. Hu, C. Cui, C. Shi, Z.-S. Wu, J. Yang, R. Cheng, T. Guang, H. Wang, H. Lu and X. Wang, *ACS Nano*, 2019, **13**, 6899–6905.
- 3 S. Zhou, S. Liu, W. Chen, Y. Cheng, J. Fan, L. Zhao, X. Xiao, Y.-H. Chen, C.-X. Luo, M.-S. Wang, T. Mei, X. Wang, H.-G. Liao, Y. Zhou, L. Huang and S.-G. Sun, *ACS Nano*, 2021, **15**, 13814–13825.
- 4 S. Lee, J. Choi, M. Kim, J. Park, M. Park and J. Cho, *Chem. Sci.*, 2022, **13**, 6159–6180.
- 5 A. Ransil and A. M. Belcher, *Nat. Commun.*, 2021, **12**, 6494.
- 6 J. S. Sanchez, J. Xu, Z. Xia, J. Sun, L. E. Asp and V. Palermo, *Compos. Sci. Technol.*, 2021, **208**, 108768.
- 7 J. S. Sanchez, A. Pendashteh, J. Palma, M. Anderson and R. Marcilla, *Electrochim. Acta*, 2018, **279**, 44–56.
- 8 Y. Sun, J. Ma, X. Yang, L. Wen, W. Zhou and J. Geng, *J. Mater. Chem. A*, 2020, **8**, 62–68.
- 9 Z. Bo, J. Yang, H. Qi, J. Yan, K. Cen and Z. Han, *Energy Storage Mater.*, 2020, **31**, 64–71.
- 10 X. Wu, H. Wu, B. Xie, R. Wang, J. Wang, D. Wang, Q. Shi, G. Diao and M. Chen, *ACS Nano*, 2021, **15**, 14125–14136.
- 11 Z. Wang, Z. Xu, H. Huang, X. Chu, Y. Xie, D. Xiong, C. Yan, H. Zhao, H. Zhang and W. Yang, *ACS Nano*, 2020, **14**, 4916–4924.
- 12 S. Subramanian, M. A. Johnny, M. M. Neelanchery and S. Ansari, *IEEE Trans. Power Electronics*, 2018, **33**, 10410–10418.
- 13 W. Zhao, M. Jiang, W. Wang, S. Liu, W. Huang and Q. Zhao, *Adv. Funct. Mater.*, 2021, **31**, 2009136.
- 14 X. Cao, B. Zheng, X. Rui, W. Shi, Q. Yan and H. Zhang, *Angew. Chem., Int. Ed.*, 2014, **53**, 1404–1409.
- 15 J. Sun, M. Sadd, P. Edenborg, H. Gronbeck, P. H. Thiesen, Z. Xia, V. Quintano, R. Qiu, A. Matic and V. Palermo, *Sci. Adv.*, 2021, **7**, eabf0812.
- 16 L. Xiao, J. Sun, L. Liu, R. Hu, H. Lu, C. Cheng, Y. Huang, S. Wang and J. Geng, *ACS Appl. Mater. Interfaces*, 2017, **9**, 5382–5391.
- 17 J. Sun, D. Meng, S. Jiang, G. Wu, S. Yan, J. Geng and Y. Huang, *J. Mater. Chem.*, 2012, **22**, 18879–18886.
- 18 A. Iakunkov, J. Sun, A. Rebrikova, M. Korobov, A. Klechikov, A. Vorobiev, N. Boulanger and A. V. Talyzin, *J. Mater. Chem. A*, 2019, **7**, 11331–11337.
- 19 J. Sun, L. Xiao, D. Meng, J. Geng and Y. Huang, *Chem. Commun.*, 2013, **49**, 5538–5540.
- 20 A. Klechikov, J. Sun, I. A. Baburin, G. Seifert, A. T. Rebrikova, N. V. Avramenko, M. V. Korobov and A. V. Talyzin, *Nanoscale*, 2017, **9**, 6929–6936.
- 21 A. Klechikov, J. Sun, A. Vorobiev and A. V. Talyzin, *J. Phys. Chem. C*, 2018, **122**, 13106–13116.
- 22 A. Klechikov, S. You, L. Lackner, J. Sun, A. Iakunkov, A. Rebrikova, M. Korobov, I. Baburin, G. Seifert and A. V. Talyzin, *Carbon*, 2018, **140**, 157–163.
- 23 J. Sun, A. Iakunkov, A. T. Rebrikova and A. V. Talyzin, *Nanoscale*, 2018, **10**, 21386–21395.
- 24 J. Sun, F. Morales-Lara, A. Klechikov, A. V. Talyzin, I. A. Baburin, G. Seifert, F. Cardano, M. Baldrighi, M. Frascioni and S. Giordani, *Carbon*, 2017, **120**, 145–156.
- 25 L. Mao, H. Park, R. A. Soler-Crespo, H. D. Espinosa, T. H. Han, S. T. Nguyen and J. Huang, *Nat. Commun.*, 2019, **10**, 3677.
- 26 J. Sun, L. Xiao, S. Jiang, G. Li, Y. Huang and J. Geng, *Chem. Mater.*, 2015, **27**, 4594–4603.
- 27 J. Sun, A. Klechikov, C. Moise, M. Prodana, M. Enachescu and A. V. Talyzin, *Angew. Chem., Int. Ed.*, 2018, **57**, 1034–1038.
- 28 C. Yang, S. Yu, C. Lin, F. Lv, S. Wu, Y. Yang, W. Wang, Z.-Z. Zhu, J. Li, N. Wang and S. Guo, *ACS Nano*, 2017, **11**, 4217–4224.
- 29 J. Memon, J. Sun, D. Meng, W. Ouyang, M. A. Memon, Y. Huang, S. Yan and J. Geng, *J. Mater. Chem. A*, 2014, **2**, 5060–5067.
- 30 J. Geng and H.-T. Jung, *J. Phys. Chem. C*, 2010, **114**, 8227–8234.



- 31 A. Kovtun, A. Candini, A. Vianelli, A. Boschi, S. Dell'Elce, M. Gobbi, K. H. Kim, S. L. Avila, P. Samori, M. Affronte, A. Liscio and V. Palermo, *ACS Nano*, 2021, **15**, 2654–2667.
- 32 J. Sun, M. A. Memon, W. Bai, L. Xiao, B. Zhang, Y. Jin, Y. Huang and J. Geng, *Adv. Funct. Mater.*, 2015, **25**, 4334–4343.
- 33 J. S. Sanchez, Z. Xia, N. Patil, R. Grieco, J. Sun, U. Klement, R. Qiu, M. Christian, F. Liscio, V. Morandi, R. Marcilla and V. Palermo, *Small*, 2022, **18**, 2106403.
- 34 J. C. Stallard, L. Wheatcroft, S. G. Booth, R. Boston, S. A. Corr, M. F. L. De Volder, B. J. Inkson and N. A. Fleck, *Joule*, 2022, **6**, 984–1007.
- 35 J. Xu, G. Yuan, Q. Zhu, J. Wang, S. Tang and L. Gao, *ACS Nano*, 2018, **12**, 4529–4535.
- 36 K. S. Kumar, N. Choudhary, Y. Jung and J. Thomas, *ACS Energy Lett.*, 2018, **3**, 480–495.
- 37 M. A. Memon, W. Bai, J. Sun, M. Imran, S. N. Phulpoto, S. Yan, Y. Huang and J. Geng, *ACS Appl. Mater. Interfaces*, 2016, **8**, 11711–11719.
- 38 Z. Xia, V. Mishukova, S. Sollami Delekta, J. Sun, J. S. Sanchez, J. Li and V. Palermo, *Nanoscale*, 2021, **13**, 3285–3294.
- 39 Z. Liu, Z. Chen, C. Wang, H. I. Wang, M. Wuttke, X.-Y. Wang, M. Bonn, L. Chi, A. Narita and K. Muellen, *J. Am. Chem. Soc.*, 2020, **142**, 17881–17886.
- 40 Y. Wang, J. Zhao, J. Qu, F. Wei, W. Song, Y.-G. Guo and B. Xu, *ACS Appl. Mater. Interfaces*, 2016, **8**, 26008–26012.
- 41 A. Y. Kozmenkova, E. Y. Kataev, A. I. Belova, M. Arnati, L. Gregoratti, J. Velasco-Velez, A. Knop-Gericke, B. Senkovsky, D. V. Vyalikh, D. M. Itkis, Y. Shao-Horn and L. V. Yashina, *Chem. Mater.*, 2016, **28**, 8248–8255.
- 42 J. Hou, W. Wang, P. Feng, K. Wang and K. Jiang, *J. Power Sources*, 2020, **453**, 227879.
- 43 G. Wang, F. Yi, J. Zhong, A. Gao, C. Liu, Q. Li, D. Shu and J. Ling, *ACS Appl. Mater. Interfaces*, 2022, **14**, 34637–34648.
- 44 A. Pendashteh, J. S. Sanchez, J. Palma, M. Anderson and R. Marcilla, *Energy Storage Mater.*, 2019, **20**, 216–224.
- 45 J. S. Sanchez, R. Ruben Maca, A. Pendashteh, V. Etacheri, V. A. de la Pena O'Shea, M. Castillo-Rodriguez, J. Palma and R. Marcilla, *Catal. Sci. Technol.*, 2020, **10**, 1444–1457.
- 46 Z. Xia, F. Leonardi, M. Gobbi, Y. Liu, V. Bellani, A. Liscio, A. Kovtun, R. Li, X. Feng, E. Orgiu, P. Samori, E. Treossi and V. Palermo, *ACS Nano*, 2016, **10**, 7125–7134.
- 47 J. Sun, J.-Y. Hwang, P. Jankowski, L. Xiao, J. S. Sanchez, Z. Xia, S. Lee, A. V. Talyzin, A. Matic, V. Palermo, Y.-K. Sun and M. Agostini, *Small*, 2021, **17**, 2007242.
- 48 Y. Ding, Y. Li, M. Wu, H. Zhao, Q. Li and Z.-S. Wu, *Energy Storage Mater.*, 2020, **31**, 470–491.
- 49 E. Pomerantseva and Y. Gogotsi, *Nat. Energy*, 2017, **2**, 17089.
- 50 C. Zhang, S.-H. Park, A. Seral-Ascaso, S. Barwich, N. McEvoy, C. S. Boland, J. N. Coleman, Y. Gogotsi and V. Nicolosi, *Nat. Commun.*, 2019, **10**, 849.
- 51 C. Ma, M.-G. Ma, C. Si, X.-X. Ji and P. Wan, *Adv. Funct. Mater.*, 2021, **31**, 2009524.

